View metadata, citation and similar papers at core.ac.uk
brought to you by CORE
provided by National Tsing Hua University Institutional Repository

Study of Magnetic Properties and Local Structures in Discontinuous-CoFe–ZnO Multilayers

H. S. Hsu, J. C. A. Huang, Lance Horng, C. H. Lee, Y. H. Huang, Y. F. Liao, and M. Z. Lin

***Abstract*—In this study, we have investigated the magnetic properties and local structures of discontinuous-$Co_{70}Fe_{30}$(x Å)–ZnO multilayers (MLs). With the variation of $Co_{70}Fe_{30}$ nominal thickness, the phase transition from diluted magnetic semiconductor (DMS) phase, $x = 1$ ML, to granular phase, $x = 5$, and 9 MLs, is indicated from the measurements of magnetization versus temperature behavior and extended X-ray absorption fine structure (EXAFS) on Co or Fe K-edge. The analysis of EXAFS at Zn K-edge shows the reduction of Co coordination numbers with the increasing CoFe thickness. This result demonstrates that the CoFe grain size plays an important role in the formation of DMS and is greatly critical for multilayer growth technique.**

***Index Terms*—Diluted magnetic semiconductor (DMS), discontinuous multiplayer, extended X-ray absorption fine structure (EXAFS).**

I. Introduction

DILUTED MAGNETIC semiconductors (DMSs) have been of much interest and studied extensively since Dietl *et al.* [1] predicted room temperature (RT) ferromagnetism can be induced by doping transition metal (TM) elements into host semiconductors. Especially, TM-doped ZnO has been investigated as a promising DMS for implementing spintronics and optoelectronics device [2]. In spite of TM atomic substitution for Zn^{2+} ions, the origin of RT ferromagnetism remains controversial. Most of the studies emphasized the magnetic elements concentration in the host semiconductor [3], but the grain size effect of doping magnetic element in fabrication process has not been particularly discussed.

In this paper, we investigate the magnetic properties and local structures of $Co_{70}Fe_{30}$–ZnO multilayers (MLs). Here, the inserted CoFe layers are discontinuous because the thickness (<1 nm) is below the minimum value of a continuous film. By varying the deposition thickness, the grain size distribution of $Co_{70}Fe_{30}$ can be controlled [4], where CoFe was chosen to study the difference of reaction in ZnO matrix between Co and Fe atom. The magnetic origin relating to the local structures surrounding Co and Fe are discussed. The size effect of the magnetic elements is also studied by extended X-ray absorption fine structure (EXAFS) spectra at Zn K-edge. We present our study on the variation of CoFe grain size to understand the related mechanism of DMS.

Manuscript received August 21, 2004. This work was supported in part by the Taiwan National Science Foundation under Grant NSC 92-2120-M-006-006.

H. S. Hsu is with the Department of Physics, National Cheng Kung University, Tainan 701, Taiwan, R.O.C. (e-mail: apiece1977@yahoo.com.tw).

J. C. A. Huang is with the Department of Physics, National Cheng Kung University, Tainan 701, Taiwan, R.O.C. and also with the Department of Applied Physics, National University of Kaohsiung, Kaohsiung 003, Taiwan, R.O.C. (e-mail: jcahuang@mail.ncku.edu.tw).

L. Horng is with the Department of Physics, National Changhua University of Education, Changhua 500, Taiwan, R.O.C. (e-mail: phlhorng@cc.ncue.edu.tw).

C. H. Lee, Y. H. Huang, Y. F. Liao, and M. Z. Lin are with the Department of Engineering and System Science, National Tsing Hua University, Hsinchu 300, Taiwan, R.O.C. (e-mail: chlee@ess.nthu.edu.tw).

Digital Object Identifier 10.1109/TMAG.2004.842085

II. Experiment

We have prepared [discontinuous-$Co_{70}Fe_{30}$ (x Å)–ZnO (20 Å)]$_{25}$ multilayers by ion-beam sputtering with a base pressure of 8×10^{-8} torr. The nominal thickness of $Co_{70}Fe_{30}$ layers were $x = 1, 5,$ and 9. Sputtering was executed in an atmosphere of 2×10^{-4} torr with Ar^+ ion beam acting alternatively on CoFe and ZnO targets. All films were deposited on Al_2O_3 (0001) single crystal substrates for good epitaxial structure. The deposition rate was calibrated to achieve uniform values of 0.2 Å/s for ZnO and 0.5 Å/s for CoFe. Measurements of the magnetization (M) as a function of magnetic field (H) and temperature (T) were characterized with a superconducting quantum interference device (SQUID) magnetometer over a temperature range of 6 K–350 K. In order to investigate the electronic states and local structure of ZnO–CoFe MLs, X-ray absorption spectroscopy on Co, Fe, and Zn K-edges was carried out at the wigger beamline of the Synchrotron Radiation Research Center, Hsinchu, Taiwan.

III. Results and Discussion

Fig. 1 shows the magnetization versus applied field (M–H) curves of the three MLs measured at 300 K. Magnetic hysteresis loops were observed for $x = 1$ and 9 MLs. In contrast, paramagnetic linear relation appears for $x = 5$ ML. Note that the coercivity of $x = 1$ ML is much larger than $x = 9$ ML. It implies the origin of RT ferromagnetism between $x = 1$ and 9 MLs may be different, as discussed in the following.

Fig. 2 displays the zero-field-cooling (ZFC) and field-cooling (FC) magnetization measurements as a function of temperature (M–T) in a low field of 50 Oe for the $x = 1, 5,$ and 9 MLs. For $x = 1$ ML, the FC magnetization remains almost constant and does not decrease to zero up to 350 K. Besides, the peak which is a signature for blocking temperature does not appear in the ZFC curve for $x = 1$ ML. This suggests that the CoFe atoms are dissolved into ZnO matrix and forms DMS without any formation of magnetic clusters.

In contrast to $x = 1$ ML, both $x = 5$ and 9 MLs show magnetic blocking phenomenon in their ZFC curves. It clearly evidences the presence of magnetic clusters in ZnO matrix for $x = 5$ and $x = 9$ MLs. Note that T_B moves to higher temperature as CoFe layer increased from $x = 5$ ($T_B = 18$ K) to

0018-9464/$20.00 © 2005 IEEE

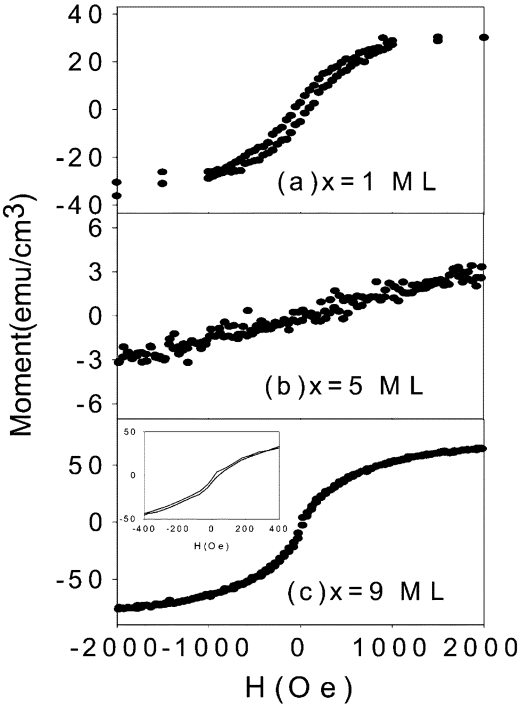

Fig. 1. Magnetization of the multilayers [ZnO(20 Å)–$Co_{70}Fe_{30}$(x Å)]$_{25}$ as a function of applied magnetic field at 300 K for (a) $x = 1$, (b) $x = 5$, and (c) $x = 9$ MLs. The inset is the zoom in figure of (c).

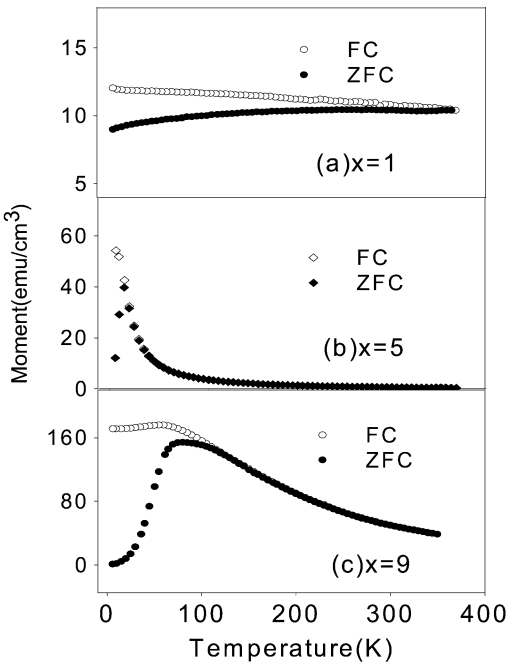

Fig. 2. ZFC (solid symbol)-FC (hollow symbol) M–T curve in a field of 50 Oe for (a) $x = 1$, (b) $x = 5$, and (c) $x = 9$ MLs.

$x = 9$ ($T_B = 80$ K), suggesting that the average size of clusters increases with the CoFe nominal thickness. The FC curve for $x = 5$ ML displays the typical Curie–Weiss behavior for disordered granular systems and the magnetization approaches to zero at RT. The linear relation of M–H loop in Fig. 1(b) is characteristic of the predominant paramagnetic phase contributed by blocked magnetic nanoparticles. The M–T behavior

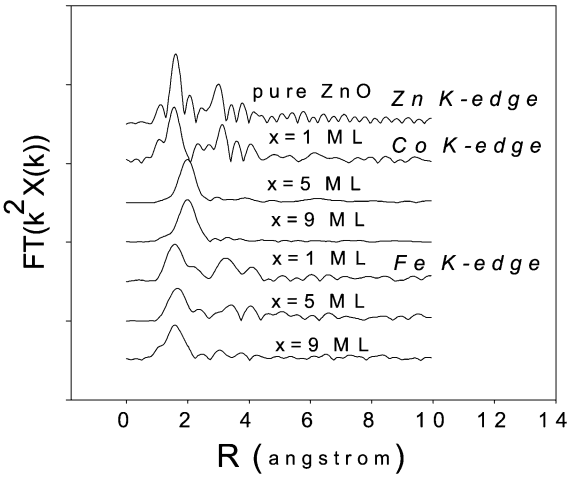

Fig. 3. Fourier transform of EXAFS for $x = 1, 5, 9$ MLs at Co, Fe K-edge, and ZnO at Zn K-edge, respectively.

of $x = 9$ ML is similar to $x = 5$ ML even if the M–H behaviors at RT are different. The RT ferromagnetism for $x = 9$ ML should be caused by the magnetic clusters, in contrast to the intrinsic DMS property for $x = 1$ ML.

Fig. 3 compares the radial distribution function (RDF), the Fourier transforms amplitude from EXAFS data on Co, Fe, and Zn K-edges for $x = 1, 5, 9$ MLs and pure ZnO. For $x = 1$ ML, the interatomic distances for the two major peaks of the film are essentially the same as undoped ZnO both on Co and Fe K-edge. The first and second major peaks are corresponding to the nearest oxygen and Zn (or Co, Fe) atoms from a specific Co (Fe) atom. Accordingly, the RDF of $x = 1$ ML reveals that most Co (Fe) atoms substitute for Zn atoms without precipitating magnetic clusters. It further supports that the origin of RT ferromagnetism for $x = 1$ ML is due to an intrinsic DMS effect. For $x = 5$ ML, essentially only one major peak has been observed at Co K-edge, indicating in average Co atoms locate at 2 Å from nearest Co atoms, or the formation of Co metal clusters. On the other hand, the RDF of Fe K-edge for $x = 5$ ML reveals only a nearest-neighbor (oxygen) shell and does not have any long-range structural order surrounding with Fe atoms. These results reveal the Co and Fe atoms play different contribution when precipitate in ZnO matrix. Similar EXAFS results were obtained for $x = 9$ ML. Therefore, the magnetic blocking behavior for $x = 5$ and 9 MLs could be mainly caused by Co clusters, not by Fe cluster. Using the literature values of T_B versus size [5], we estimate the average size of the Co nanoparticles in our samples are about 1 nm for $x = 5$ ML and about 8 nm for $x = 9$ ML. The RT ferromagnetism for $x = 9$ ML could originate from the large unblocked Co nanoparticles.

Fig. 4 shows the Fourier transforms of $x = 1, 5$, and 9 MLs from the Zn K-edge EXAFS data. The two pronounced peaks for all samples are located at the resemble R values. It is noted that the magnitudes of the second shell peaks ($\sim$3.0 Å) are slightly reduced with increasing the CoFe thickness. It means that the second nearest neighbor surrounding with Zn atoms (Zn, Co, or Fe) is different for $x = 1, 5$, and 9 MLs. The quantitative local structure information was obtained by curve fitting (solid curves) from theoretical models generated by the well-known

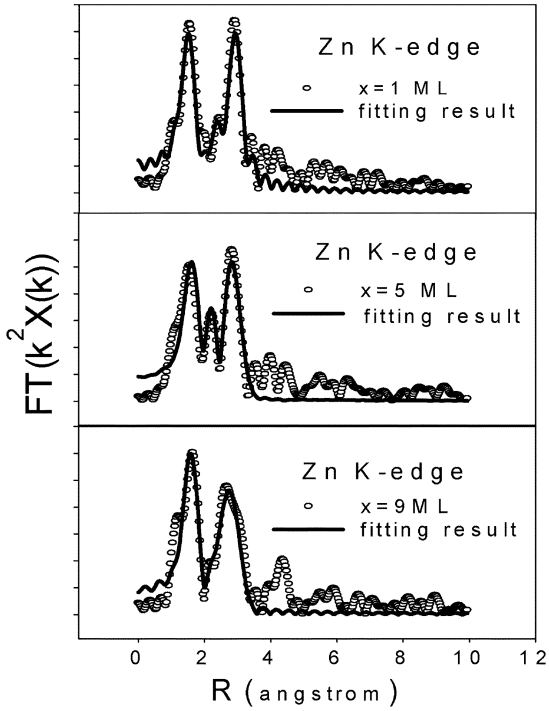

Fig. 4. Fourier transforms of EXAFS at Zn K-edge (hollow symbols) and fitting results (solid curves) from FEFF code for (a) $x = 1$, (b) $x = 5$, and (c) $x = 9$ MLs.

TABLE I
RESULTS OF FITS TO $x = 1, 5$, AND 9 MLs. Zn-O PAIR IS THE FIRST COORDINATION SHELL AND Zn-Zn PAIR IS THE SECOND COORDINATION SHELL. N IS THE COORDINATION NUMBER, R IS THE DISTANCE BETWEEN CENTERED Zn ATOMS AND COORDINATION ATOMS, AND σ^2 IS THE MEAN SQUARE DISORDER AT ROOM TEMPERATURE

Sample		*R*(Å)±2%	N_c±20%	σ^2(Å^2)±20%
x=1 ML	1st-shell	Zn-O 1.93	Ox 4.39	0.0049
	2nd-shell	Zn-Zn 3.31	Znx9.71	0.0089
		Zn-Co 3.12	Cox2.83	0.0026
		Zn-Fe 2.97	Fex0.10	0.0428
x=5 ML	1st-shell	Zn-O 1.98	Ox 3.36	0.0045
	2nd-shell	Zn-Zn 3.44	Znx13.19	0.0123
		Zn-Co 2.82	Cox0.52	0.0002
		Zn-Fe 3.47	Fex0.58	0.0428
x=9 ML	1st-shell	Zn-O 1.98	Ox 3.36	0.0027
	2nd-shell	Zn-Zn 3.44	Znx12.61	0.0131
		Zn-Co 2.82	Cox0.64	0.0118
		Zn-Fe 3.47	Fex0.57	0.0376

FEFF program. The solid curves in Fig. 4 are obtained by the best fit of the experimental data, which reveal reasonably good agreement of the theoretical model with the data. For convenience, the fitting results are summarized in Table I.

For the first coordination shell, all three samples have the same coordination number ($N_c \sim 4$) within the error bar for the Zn-O pair. For the second coordination shell, the Fe coordination numbers are less than 1 for all MLs, particularly clear for $x = 1$ ML. The origin of low Fe solubility is not clear so far. Fe may be stable in the trivalent state in ZnO, resulting in the low solubility limit [6]. Besides, $x = 1$ ML shows N_c of 2.83 Co atoms, while $x = 5$ and $x = 9$ MLs have only 0.52 and 0.64 Co atoms, respectively. The reduction of Co coordination numbers results in a less incorporation in ZnO matrix without ever reaching to saturation condition. This indicates that the increase of CoFe nominal thickness (x) does not increase in magnetic doping concentration if the magnetic elements exceed a critical thickness ($x > 1$). These results suggest that the structure and magnetism of discontinuous-CoFe/ZnO multilayers is very sensitive to nominal CoFe thickness because of the variation in solubility. The control of inserting magnetic grain size distribution can stabilize or destroy the DMS phase.

IV. CONCLUSION

We have performed systematical study of magnetic properties and local structures of Co, Fe, and Zn in discontinuous-CoFe/ZnO multilayers. By varying in $Co_{70}Fe_{30}$ nominal thickness, the two-step magnetic phase transition from RT ferromagnetism ($x = 1$), paramagnetism ($x = 5$) and to RT ferromagnetism ($x = 9$) have been observed. The measurements on M–T behavior and EXAFS on Co (Fe) edge further indicate that the observed RT ferromagnetism for $x = 1$ ML originates from an intrinsic DMS phase, whereas the RT ferromagnetism for $x = 9$ ML is caused by large unblocked Co nanoparticles. This result could be associated with varying dimensionality between magnetic clusters, evidenced by the quantitative local structure information at Zn K-edge.

REFERENCES

[1] K. Sato and H. Katayama-Yoshida, "Stabilization of ferromagnetic states by electron doping in Fe-, Co-or Ni-doped ZnO," *Jpn. J. Appl. Phys.*, pt. 2, vol. 40, pp. L334–L336, 2001.

[2] S. A. Wolf, D. D. Awschalom, R. A. Buhrman, J. M. Daughton, S. von Molnar, M. L. Roukes, A. Y. Chthekanova, and D. M. Treger, "Spintronics: A spin-based electronics vision for the future," *Science*, vol. 294, pp. 1488–1495, 2001.

[3] J. H. Park, M. G. Kim, H. M. Jang, S. Ryu, and Y. M. Kim, "Co-metal clustering as the origin of ferromagnetism in co-doped ZnO thin films," *Appl. Phys. Lett.*, vol. 84, pp. 1338–1340, 2004.

[4] G. N. Kakazei, Y. G. Pogorelov, A. M. L. Lopes, J. B. Sousa, S. Cardoso, P. P. Freitas, M. M. Prerira de Azevedo, and E. Snoeck, "Tunnel magnetoresistance and magnetic ordering in ion-beam sputtered $Co_{80}Fe_{20}$–Al_2O_3 discontinuous multilayers," *J. Appl. Phys*, vol. 90, pp. 4044–4048, 2001.

[5] J. P. Chen, C. M. Sorensen, K. J. Klabunde, and G. C. Hadjipanayis, "Enhanced magnetization of nanoscale colloidal cobalt particles," *Phys. Rev. B, Condens. Matter*, vol. 51, pp. 11 527–11 532, 1995.

[6] R. Heitz, A. Hoffmann, and I. Broser, "Fe^{3+} center in ZnO," *Phys. Rev. B, Condens. Matter*, vol. 45, pp. 8977–8988, 1992.